SOFT ROBOTICS

Bioinspired microrobots

Stefano Palagi[1]* *and Peer Fischer*[1,2]*

Abstract | Microorganisms can move in complex media, respond to the environment and self-organize. The field of microrobotics strives to achieve these functions in mobile robotic systems of sub-millimetre size. However, miniaturization of traditional robots and their control systems to the microscale is not a viable approach. A promising alternative strategy in developing microrobots is to implement sensing, actuation and control directly in the materials, thereby mimicking biological matter. In this Review, we discuss design principles and materials for the implementation of robotic functionalities in microrobots. We examine different biological locomotion strategies, and we discuss how they can be artificially recreated in magnetic microrobots and how soft materials improve control and performance. We show that smart, stimuli-responsive materials can act as on-board sensors and actuators and that 'active matter' enables autonomous motion, navigation and collective behaviours. Finally, we provide a critical outlook for the field of microrobotics and highlight the challenges that need to be overcome to realize sophisticated microrobots, which one day might rival biological machines.

Microorganisms are simple, single-celled organisms at the microscale that possess machinery that enables them to actively swim, to sense and act on their environment, and to autonomously and collectively respond to external stimuli[1]. Remarkably, microorganisms achieve their sophisticated behaviours without a central processor or nervous system by relying on complex networks of biophysical and chemical sensing-action loops. It has been a long-sought goal in the field of microrobotics to create artificial microrobots and microscopic machines that achieve the behavioural sophistication of microorganisms[2]. Such microscale robots would be especially interesting for minimally invasive medical applications[3,4].

Building and operating microscopic robots is not simply a matter of miniaturizing existing robotic technologies. Macroscale robots are machines that consist of arrays of separate sensors, actuators and programmable control units, but such components are challenging to realize and integrate in a robotic system at the microscale. However, mimicking the design principle of microorganisms will allow for the engineering of micrometre-sized machines with robotic functionalities, so that they may autonomously or semi-autonomously perform specific tasks in complex environments.

In this Review, we show that the realization of sophisticated biomimetic robotic functionalities in artificial microsystems benefits from soft, responsive and active materials. We discuss how different locomotion mechanisms of microorganisms can be mimicked with soft materials and how smart materials enable a microrobot to perceive the environment and to respond to it. We also examine energy-consuming 'active' material systems that exhibit autonomous and collective behaviours reminiscent of biological organisms.

[1]*Max Planck Institute for Intelligent Systems, Stuttgart, Germany.*

[2]*Institut für Physikalische Chemie, Universität Stuttgart, Stuttgart, Germany.*

**e-mail: palagi@is.mpg.de; fischer@is.mpg.de*

https://doi.org/10.1038/s41578-018-0016-9

Controlled bioinspired propulsion

Many suggested applications of microrobots for minimally invasive medical procedures and targeted drug delivery require locomotion in fluids. Microrobots that can controllably move in liquid environments can be developed by mimicking the propulsion strategies of swimming microorganisms.

Moving in liquids at the microscale is fundamentally different from swimming at the macroscale[5]. For an organism or an artificial machine of length L, swimming at speed U in a fluid with density ρ and dynamic viscosity μ, the Reynolds number $Re = \rho LU/\mu$ corresponds to the ratio of inertial to viscous forces. In water, Re is about 10^6 for a human swimmer, 10^2 for a small fish, 10^{-1} for a paramecium and 10^{-4} for a bacterium[5]. The practical consequence is that for micrometre-sized organisms and machines, inertial forces are negligible compared with viscous forces. The fluid has no memory and the flow is instantaneous; thus, in Newtonian fluids, such as water, time-reversible motion does not lead to net propulsion, which is known as 'the scallop theorem' (REF.[5]). Nonetheless, only urine and cerebrospinal fluid have Newtonian behaviour among biological fluids. Blood, synovial fluid, mucus, vitreous humour, saliva, and others are all non-Newtonian[6]. In non-Newtonian fluids, the scallop theorem does not apply, and even simple time-reversible body shape changes can lead to effective propulsion[7]. In addition, many biological media contain networks of macromolecules that

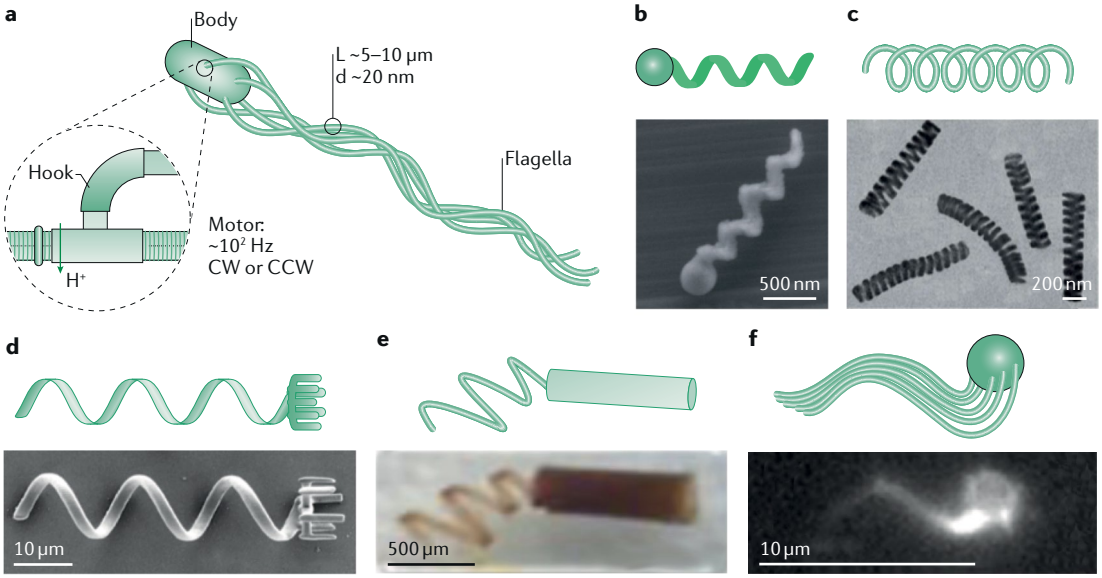

Fig. 1 | **Propulsion of helical microstructures.** Bacteria possess one or more flagella that spontaneously form a helical bundle that propels the cell body forward (part **a**). Flagella are actuated at the base by a rotary motor, connected to the flagellum by a flexible hook[100]. Rigid magnetic helical micropropellers can be fabricated by vapour deposition of silica and nickel (part **b**), template-assisted electrodeposition of palladium and nickel (part **c**) and two-photon lithography of photoresist polymers subsequently coated with nickel (part **d**). Self-assembled flexible magnetic micropropellers can be engineered by magnetically programmed self-folding of layered hydrogel-based structures (part **e**) and by assembly of DNA-based flagella on a magnetic microparticle (part **f**). CCW, anticlockwise; CW, clockwise. Panel **b** is reproduced with permission from REF.[16], American Chemical Society. Panel **c** is adapted with permission from REF.[18], Royal Society of Chemistry. Panel **d** is adapted with permission from REF.[19], John Wiley and Sons. Panel **e** is adapted with permission from REF.[23], IEEE. Panel **f** is adapted from REF.[24], CC-BY-4.0.

hinder movement[8] and require innovative strategies for microrobotic locomotion.

Most microorganisms, as well as spermatozoa, swim using cilia and flagella, which are appendages that execute non-reciprocal propulsive motions, namely, corkscrew-like movements or beating and waving[9]. Such propulsive appendages can be mimicked to enable microrobots to move in liquids[10], for example, through the use of magnetic materials and external magnetic fields[11]. The shape and mechanical properties of these artificial propellers are key to achieve locomotion of microrobots in simple and complex fluidic environments.

Helical propellers. Bacteria swim by rotating propellers called flagella. Bacterial flagella consist of thin, passive helical filaments that are actuated at the base by molecular rotary motors[12] (FIG. 1a). In some bacteria, for example, Spirochaetes, the body itself has a helical shape[13]. The rotation of the flagellum causes corkscrew-like propulsion owing to rotation–translation coupling[5]. Rotary motors are commonly used in macroscale machines; however, realizing them at the microscale is challenging. Therefore, artificial helical micropropellers inspired by bacterial flagella are typically driven by an external rotating magnetic field, which mitigates the need for an on-board rotary micromotor. In addition, variation of the axis of rotation of the magnetic field enables steering. The propulsion speed of such artificial microstructures strongly depends on their helical shape[14].

Rigid magnetic microhelices can be fabricated by a variety of techniques, such as self-scrolling, that is, the rolling of thin material layers into specific shapes by controlling the internal stress[15]; glancing angle deposition (GLAD) (FIG. 1b), which can be used to grow billions of microhelices[16] or nanohelices[17] in parallel on a tilted, rotating stage through a physical vapour deposition process; template-assisted electrodeposition[18] (FIG. 1c); direct laser writing (DLW), which is a 3D lithographic process based on two-photon polymerization of a photoresist[19] (FIG. 1d); and the coating of biological helical templates[20,21]. Self-scrolling, DLW and coating of biological templates enable the fabrication of helical structures with lengths ranging from a few to several tens of micrometres, whereas template-assisted electrodeposition and GLAD enable the fabrication of helices of sub-micrometre length. The micropropellers contain a ferromagnetic material, which is diametrically magnetized to allow rotation, and thus propulsion, by an external rotating homogeneous magnetic field.

Artificial helical micropropellers are an extremely effective solution for the propulsion of microrobots in water-like, Newtonian fluids. However, locomotion in complex biological fluids requires additional strategies owing to the mesoporous macromolecular structure of biological fluids. Whereas microscale propellers cannot move through these media, nanopropellers with a filament diameter of about 70 nm, which are smaller than any biological swimmer[17], can readily penetrate the mesh of the biopolymeric networks found in many tissues. Alternatively, biochemical modifications of

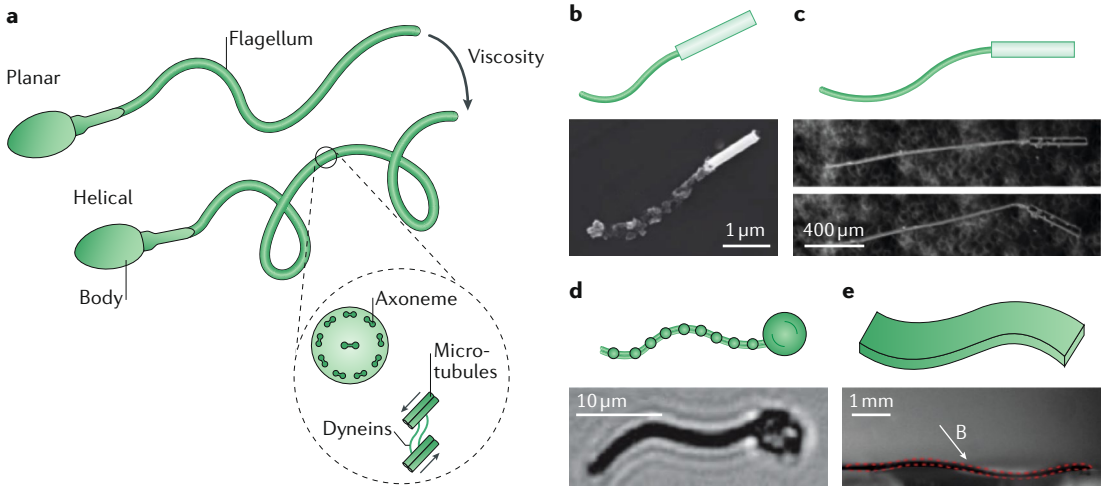

Fig. 2 | **Propulsion of flexible microstructures. a** | Sperm cells swim owing to bending waves that propagate along their long, flexible flagellum. The waveform depends on the viscosity of the surrounding fluid and can be either planar or helical. The bending of the flagellum is powered by dynein motor proteins that cause sliding of microtubule doublets in the axoneme. **b** | A microrobot with a magnetic head and a flexible nanowire tail can move in liquids once actuated by a magnetic rotating field. **c** | A sperm-shaped polydimethylsiloxane microstructure can swim because of a flexible tail actuated by cardiac cells. **d** | Propulsive travelling bending waves are generated by a combination of static and oscillating magnetic fields in a flexible chain of DNA-linked microbeads. **e** | A rotating magnetic field (B) induces travelling bending waves in a flexible sheet with a preprogrammed magnetization profile, which results in locomotion at the water–air interface. Panel **b** is adapted with permission from REF.[28], Royal Society of Chemistry. Panel **c** is adapted from REF.[30], Macmillan Publishers Limited. Panel **d** is adapted from REF.[31], Macmillan Publishers Limited. Panel **e** is adapted with permission from REF.[34], American Institute of Physics.

micropropellers enable navigation through porous protein-based gels. For example, micropropellers can be coated with urease enzymes to penetrate mucus, mimicking the strategy of *Helicobacter pylori*[22]. Urease converts urea into ammonia and thus locally increases the pH, which reversibly liquefies the mucus and facilitates its penetration. This represents just one of the countless strategies that bacteria have evolved to facilitate their own locomotion.

Bacteria are not fully rigid and exploit their flexibility for locomotion. In monotrichous (mono-flagellated) bacteria, the main source of flexibility is the hook that links the flagellum to the shaft of the motor. Microrobots can be designed with a flexible connection between the head and the tail using a self-folding magnetic hydrogel composite, mimicking the propulsion of *Caulobacter crescentus* (FIG. 1e). Such microrobots consist of a diametrically magnetized tubular head with a thin flexible chiral tail. The actuation of the flexible structure by a rotating magnetic field and its consequent movement in the fluid causes deformation at the head–tail junction and precession of the head, which influences the propulsion. Flexibility increases the motility of the microrobots when the helical trajectory of the head has the same chirality as the tail, resulting in a synergistic propulsion by the head and the tail[23]. In peritrichous (multi-flagellated) bacteria, for example, *Escherichia coli*, flagella of different lengths project out of the cell body in all directions. Thus, the bundle of flagella is generally thinner at the distal part than at the part close to the cell body, resulting in a propeller with variable stiffness. Flagella-like propellers with variable stiffness can be obtained, for example, in bacteria-mimics made of magnetic microparticles modified with flexible DNA-based flagella that spontaneously assemble into bundles upon the application of a rotating magnetic field (FIG. 1f). Bundles of flagella with decreasing stiffness towards the bundle tips result in higher swimming speed of the microrobots compared with bundles with constant stiffness[24]. These results suggest that the variable stiffness of flagella bundles has a similar role in real bacteria as well.

The flexibility of artificial flagella can be further increased, such that their shape is not fixed at the fabrication stage but determined by a complex interplay between their mechanical properties and the rheological properties of the fluid during propulsion. This strategy mimics the swimming mechanism of eukaryotic flagellates and sperm cells.

Flexible filaments. Sperm cells and many unicellular eukaryotes swim by means of flexible flagella that propagate bending waves and that are at least ten times larger (in terms of both diameter and length) than bacterial flagella[13]. The waveform of the beating eukaryotic flagella depends on the viscoelastic properties of the fluid (for example, sperm cells can switch from a planar to a helical waveform with increasing fluid viscosity)[25] (FIG. 2a). Microrobots that have a flexible tail can move in a way that resembles eukaryotic flagellated propulsion.

A flexible filament (the tail) that is actuated at one end (the head) and immersed in a viscous fluid can deform in a non-reciprocal way. The shape and propulsive performance of an actuated passive flexible tail depend on both viscous and bending forces, whose relative magnitudes are described by the sperm number $Sp = L(\xi_{\perp}\omega/A)^{1/4}$, in which L, $\xi_{\perp}$ and A are the length, transverse viscous drag and

bending stiffness of the flexible tail, respectively, and ω is the angular frequency of the driving action. The transverse viscous drag depends on dynamic viscosity μ, tail length L and diameter d, with $\xi_{\perp} = 4\pi\mu/[\log(2L/d) + C]$ (C is a constant, often 0.5, but some authors use 0.193 instead[26]). The bending stiffness also depends on the geometry and mechanical properties of the tail, with $A = EI$, in which E is the Young's modulus and I is the second moment of inertia of the tail. Therefore, the sperm number describes the swimming speed and efficiency as a function of the geometry and the mechanical properties of the flexible tail and the fluid. For $Sp \ll 1$, the bending forces dominate and the tail motion is almost reciprocal, resulting in negligible swimming speed. For $Sp \gg 1$, the viscous forces dominate, which means that the amplitude of motion rapidly decays along the tail, also resulting in inefficient swimming. Therefore, an optimal swimming performance is characterized by intermediate values of Sp[27].

The optimal value of Sp varies depending on the propulsion strategy (that is, a rotating or beating tail) and the driving action. For example, rotating tail propulsion can be obtained in a microswimmer made of a rigid magnetic nickel head and a flexible silver tail. The microswimmer, fabricated by template-directed electrodeposition and subsequent partial dissolution of the silver in hydrogen peroxide, has an optimal value of $Sp \approx 2$ (FIG. 2b). A magnetic field precessing around the propulsion direction exerts a torque on the magnetic head, which, in combination with the viscous drag of the fluid, induces bending of the flexible tail into a chiral, helical shape[28]. Alternatively, a 'flexible oar' (REF.[5]) propulsion mechanism can be achieved through oscillatory beating of the flexible tail, which, depending on the value of Sp, can result in the non-reciprocal undulation of the tail, resembling the planar waveform of sperm cells. Theoretically, sperm-inspired microrobots driven by an oscillating magnetic head[29] have an optimal swimming performance with $Sp \approx 4.3$ (REF.[26]). For sperm-shaped microswimmers made of polydimethylsiloxane (PDMS) and actuated by cardiac cells at the base of the tail (FIG. 2c), a similar optimal value of Sp has been theoretically predicted and experimentally demonstrated[30].

Passive filaments actuated at one end can therefore effectively act as propulsive appendages for microrobots. However, to mimic the locomotion of sperm cells, more complex actuation approaches are required that allow active propagation of bending waves as in the flagella of spermatozoa.

Flexible magnetic composites. Eukaryotic flagella generate bending waves through the distributed activity and self-organization of molecular motors. A sperm flagellum once severed from the cell body is still able to autonomously propagate bending waves and beat, as long as the protein machinery is intact and ATP is provided[13]. However, artificial bending microactuators are not capable of propagating bending waves because they typically perform only one-sided bending (with a positive or a negative curvature), they exhibit perfectly synchronous bending along their length (no propagation) and they need external power and control.

Propagation of bending waves in artificial systems can be achieved through magnetic actuation of flexible structures with distributed magnetization. For example, a flexible filament of a few tens of micrometres in length, consisting of a linear chain of magnetic microparticles that are linked by DNA and attached to a red blood cell, aligns with an external uniform magnetic field and is actuated by a transverse oscillating field (FIG. 2d). The red blood cell that is attached to one end of the filament breaks the symmetry of the system, thus enabling the propagation of a bending wave from the tip to the base of the filament[31]. The magnetically controlled beating of the filament propels the microrobot pulling the red blood cell body in the direction of the filament tip, which is different from the pushing action that flagella exert on the sperm cell body[32]. Multistep electrodeposition and selective etching can also be combined to fabricate undulating slender micropropellers with multiple magnetic links[33].

Alternatively, the magnetization distribution profile of a millimetre-sized flexible composite sheet of dispersed ferromagnetic powder in an elastomer matrix can be preprogrammed to actively propagate bending waves through magnetic fields (FIG. 2e). A periodic magnetization profile can be designed along the sheet to induce propagating bending waves by an external rotating magnetic field[34]. This approach enables multimodal locomotion in magnetoelastic robots at the millimetre scale[35]. To create analogous magnetic flexible composites at the microscale, elastomers can be loaded with superparamagnetic nanoparticles[36].

Rod-like magnetoelastic microstructures anchored to a surface can be used as artificial cilia, which can be collectively actuated by an external magnetic field to pump and mix fluids[37]. Cilia are hair-like appendages that are found in densely packed arrays on the surface of many eukaryotic cells, for example, in the lung to transport mucus. Cilia propel fluids by spontaneously beating with a short spatially varying lag phase[38]. By contrast, artificial magnetic mimics of cilia are actuated by a global magnetic field and thus beat in perfect synchrony, resulting in unsteady fluid propulsion. Recreating ciliary propulsion in microrobots requires controllable on-board actuators, for example, by incorporating stimuli-responsive materials.

On-board sensing and actuation

Smart soft materials comprise polymers and gels that respond to external stimuli (for example, light or temperature changes)[39]. As part of microrobots, smart materials can function as controlled actuators by using external control signals to trigger a specific material response (FIG. 3). If instead the response is elicited by an environmental cue, the material can endow the microrobot with sensing functionalities or even spontaneous behaviours. A widely used soft responsive material is poly(*N*-isopropylacrylamide) (PNIPAM). PNIPAM has a low critical solution temperature (LCST) of about 32 °C in water; thus, heating above the LCST leads to the transition from a hydrated to a dehydrated phase. Hydrogels based on PNIPAM undergo macroscopic shrinkage (de-swelling) above the LCST (FIG. 3a).

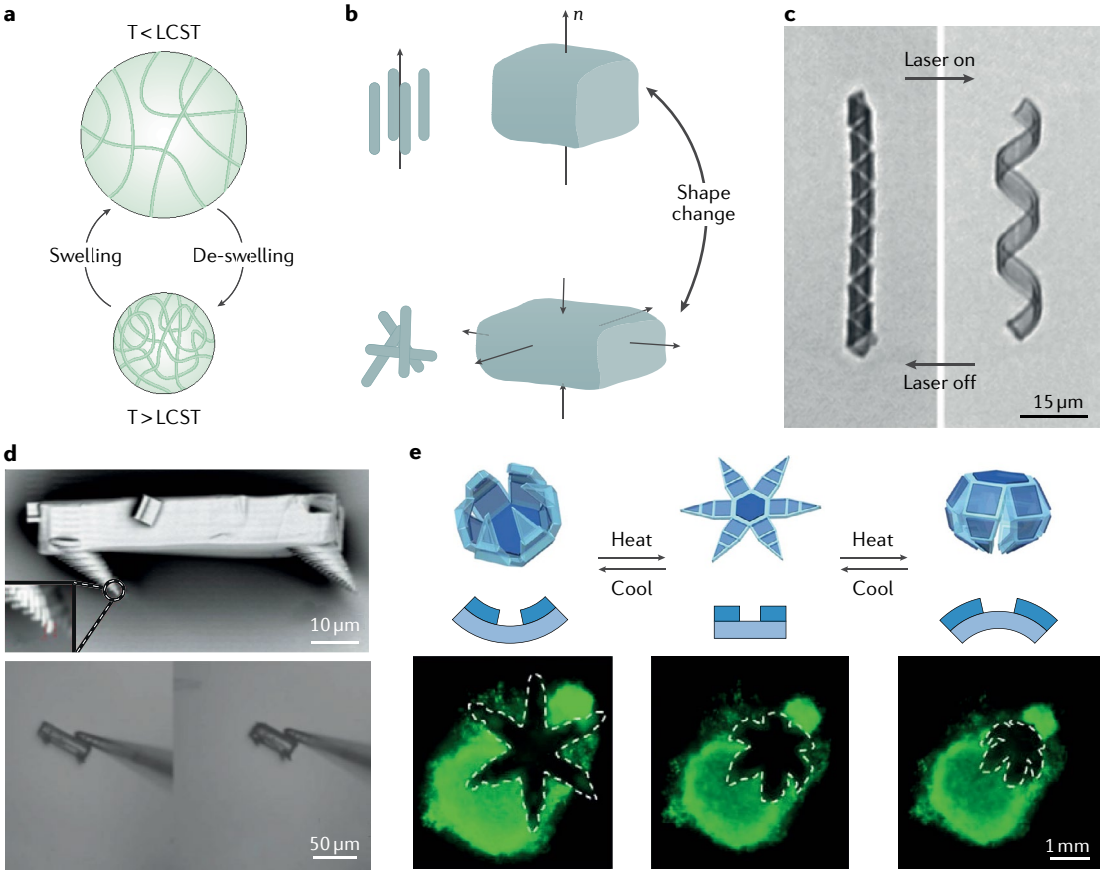

Fig. 3 | **Responsive polymers as actuators in microrobotics. a** | Poly(*N*-isopropylacrylamide) (PNIPAM) hydrogels swell and de-swell in response to temperature changes around the lower critical solution temperature (LCST). **b** | Liquid-crystal elastomers (LCEs) undergo a thermally and/or optically induced transition from a nematic (ordered) phase (*n* is the nematic director) to an isotropic (disordered) phase, accompanied by an isovolumetric shape change. **c** | Laser light can be used to power the actuation of a microribbon based on a PNIPAM hydrogel loaded with gold nanorods. **d** | A microwalker consisting of a photoresponsive LCE body and asymmetric rigid legs. **e** | A PNIPAM-based thermoresponsive gripper can capture and excise cells from a live cell fibroblast clump (green). Panel **c** is reproduced from REF.[45], CC-BY-4.0. Panel **d** is adapted with permission from REF.[48], John Wiley and Sons. Panel **e** is adapted with permission from REF.[56], American Chemical Society.

Liquid-crystal elastomers (LCEs) are another class of thermoresponsive and/or photoresponsive soft materials that have been used in mobile microrobots[40]. LCEs transition from an ordered phase (often nematic) to a disordered (isotropic) phase when the temperature increases above a critical value and/or a molecular photoswitch is activated by light. In a nematic LCE, the liquid-crystal molecules macroscopically align along a specific direction, called the nematic director. The temperature-dependent or light-dependent molecular reorientation induces an isovolumetric shape change of the material, with contraction along the nematic director and expansion in the perpendicular plane[41] (FIG. 3b). Therefore, stimuli-responsive soft materials provide microrobots with advanced functionalities and locomotion strategies[42].

Controlled locomotion. Smart soft materials can be used as on-board actuators to improve the control of microrobots or to implement different locomotion strategies. For example, soft magnetic micromachines propelled by synthetic flagella can be modified with a layer of thermoresponsive PNIPAM hydrogel, enabling a shape change in response to infrared light and thus a change in propulsion characteristics[43]. Microrobots based on smart materials can mimic how microorganisms move through body shape changes, with internally generated actuation forces controlled by external fields. For example, bell-like PNIPAM hydrogel microstructures can be fabricated by combining microfluidics with emulsion-template synthesis. Repeated temperature changes around the LCST trigger an asymmetric cycle of shrinking and swelling, enabling temperature-driven walking[44]. However, this approach requires a temperature change of the whole environment. The microrobot can be more specifically addressed by using light to trigger a material response[40].

Microrobots consisting of photoresponsive soft materials can be powered by light. For example, microribbons can be made by coating a thin (1 μm) sheet of a PNIPAM hydrogel loaded with nanorods with a 2 nm gold layer to achieve light-powered motion[45] (FIG. 3c). Plasmonic nanoparticles, resonantly excited by near-infrared light, rapidly and locally heat their immediate vicinity[46], leading to fast plasmonic heating of the PNIPAM microstructures, which triggers their non-equilibrium

actuation and thus non-reciprocal deformations. The helical microstructures then convert the non-reciprocal deformations into a net translocation in the proximity of a solid boundary[45]. Alternatively, photoresponsive LCEs can be used to achieve locomotion at small scales[47]. For example, an LCE can be microfabricated into a structure with asymmetric rigid legs, which are powered by light, to perform directional walking on pre-patterned surfaces with asymmetric friction[48] (FIG. 3d).

An advantage of light over other control mechanisms is that it provides both the temporal and spatial resolution required to selectively control the actuation of different parts of a microrobot[49]. For example, by exploiting the selective light-controlled deformation of LCEs, soft microrobots can be engineered that are able to swim, mimicking the propulsion of ciliates[42]. Ciliates are unicellular microorganisms fully covered by cilia, which self-coordinate to generate 'metachronal waves' (FIG. 4a), making ciliates fast and adaptive swimmers. Ciliary propulsion can be approximated by the 'envelope model' (REFS[50,51]), in which the coordinated action of thousands of cilia is modelled by using an effective waving surface, the envelope. By making a similar abstraction, metachronal-wave-inspired propulsion can be implemented in microrobots[52]. Travelling-wave deformations are induced in a continuous nematic LCE by a dynamic structured (or patterned) light field, resulting in the propulsion of the microrobot (FIG. 4b). The travelling-wave deformation generated in the microrobot has both transverse and longitudinal components owing to the nature of the LCE response. The relative amplitude of the two components changes with the periodicity of the light pattern, resulting in swimming in the direction parallel to the travelling wave for short-wavelength deformations and in an antiparallel direction for long-wavelength deformations. The two swimming modes resemble the symplectic and antiplectic metachrony types in ciliates[42] and can be achieved because the deformation of the microrobots is not preprogrammed in the material but controlled by light. Therefore, the monolithic microrobots behave as if they consist of many independent actuators[53], enabling the implementation of a variety of different gaits and the ability to self-propel in different environments[54] (FIG. 4b). Therefore, responsive materials facilitate the realization of sophisticated biomimetic locomotion strategies. In addition, they enable the incorporation of additional functionalities, such as cell and drug delivery.

Controlled and spontaneous delivery. The responsiveness of PNIPAM and other smart hydrogels can be exploited for the delivery of cargo. For example, cells can be captured and released by self-folded microstructures using temperature-controlled folding and unfolding, and the microstructures can move through control by magnetic fields[55]. PNIPAM-based thermomagnetic soft grippers can also be applied for cell excision[56] (FIG. 3e). Drugs and molecules can be loaded onto the microrobots and released at a specific location in response to an external trigger or an environmental cue[57]; for example, a magnetic microrobot can be made of a thermoresponsive hydrogel loaded with magnetic nanoparticles and a molecular payload, which is released on demand through heating by magnetic induction[58]. Alternatively, the payload can be released through infrared light-induced unfolding of tubular microrobots that possess a graphene oxide PNIPAM-based hydrogel layer[59].

Microrobots can also spontaneously release molecules in response to an environmental stimulus, such as a pH change, which is often associated with inflamed tissue or tumours. For example, a magnetic microrobot can be coated with a chitosan gel layer that shrinks in acidic conditions[60]. Similarly, a drug can be loaded into microbeads that are carried by a pH-responsive microgripper based on 2-hydroxyethyl methacrylate[61]. Here, the responsive materials act as both sensor and actuator, endowing the microrobot with a pre-predefined spontaneous behaviour (BOX 1). This approach can also be applied to trigger spontaneous movement, for example, by using self-oscillating gels.

Spontaneous movement. Self-oscillating gels are active soft materials that consume energy and that can be exploited to introduce specific behaviours in microrobots. They consist of PNIPAM-based copolymers that contain ruthenium tris(2,2′-bipyridine), which catalyses a self-oscillating Belousov–Zhabotinsky (BZ) reaction[62]. The BZ reaction serves as a chemical model for many self-oscillating biochemical processes, such as the self-organization of amoeba cells, and has complicated kinetics with feedback mechanisms. In the presence of specific substrate molecules, the BZ reaction proceeds and the embedded ruthenium compound spontaneously undergoes periodic oxidation and reduction reactions (chemical waves), which drive a swelling–de-swelling cycle in the gel. In a hydrogel larger than the chemical wavelength, the reaction–diffusion coupling elicits propagation of the wave, resulting in peristaltic shape changes[62] and the autonomous locomotion of centimetre-scale gel strips[63]. Self-oscillating hydrogels could potentially be used to develop amoeboid-mimicking microrobots capable of spontaneous movement; however, the long period and small amplitude of the mechanical oscillations remain challenges to overcome[64].

Amoeboid locomotion refers to a variety of cellular locomotion modes[65]. Cells, such as leukocytes or cancer cells, use amoeboid locomotion to crawl on 2D surfaces (for example, along the walls of blood vessels) and to navigate through 3D porous environments, such as the complex polymeric network of the extracellular matrix. Amoeboid locomotion is enabled by large deformations of the compliant cell body and does not require specialized appendages[13] (FIG. 4c). Implementing amoeboid locomotion in microrobots would be particularly interesting for medical applications, for example, to enable the robot to access biological tissues without using the vasculature.

Soft microrobots realizing amoeboid locomotion have not yet been developed, but some amoeba-inspired systems have been presented. For example, an amoeba-like self-oscillating polymeric fluid can be designed that undergoes autonomous sol–gel transition and thus can

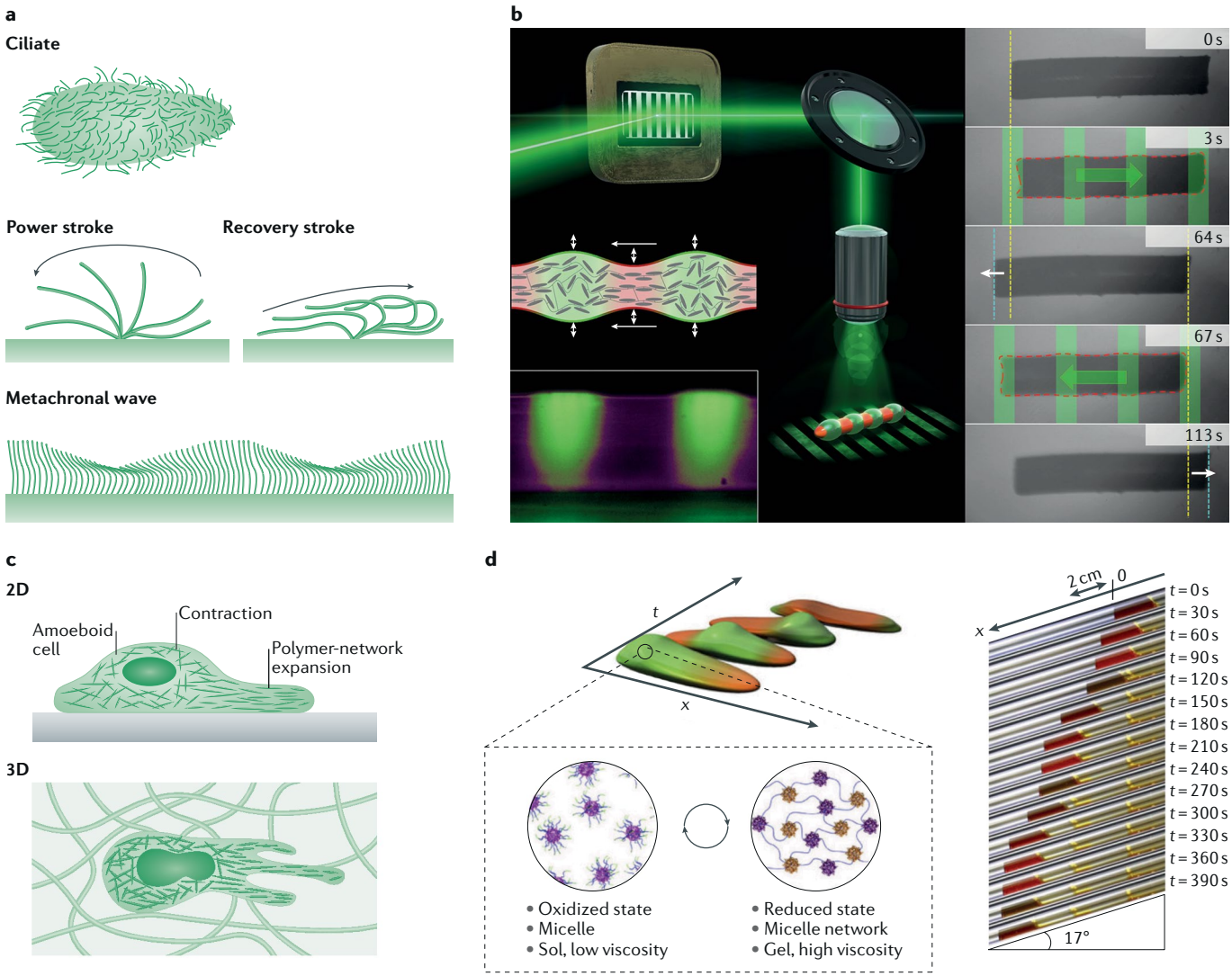

Fig. 4 | **Bioinspired locomotion by stimuli-responsive soft materials. a** | Self-coordination of cilia causes metachronal waves, that is, organism-scale propagation of waves on the surface of the cell. **b** | A soft microrobot based on a photoresponsive liquid-crystal elastomer swims by travelling-wave deformations, mimicking metachronal waves in ciliates. **c** | Amoeboid locomotion results from intracellular oscillations between contraction and polymer-network expansion, enabling cells to crawl on surfaces and through the extracellular matrix. **d** | Self-oscillating polymeric fluids undergo a periodic sol–gel transition as a micelle network forms and disassembles. A droplet of the fluid exhibits autonomous oscillating sliding resembling amoeba crawling. *t*, time. Panel **a** is adapted with permission from REF.[6], Elsevier. Panel **b** is adapted from REF.[42], Macmillan Publishers Limited. Panel **c** is adapted with permission from REF.[65], Elsevier. Panel **d** is adapted from REF.[66], CC-BY-4.0.

intermittently slide down an inclined plane[66] (FIG. 4d). Amoeba-like crawling can also be modelled by combining nanofabricated inorganic materials with biological components. For example, a material system based on lipid vesicles that contain nanoparticles, which are functionalized with actin-polymerizing proteins and packaged with actin and actin-binding proteins, is fuelled by ATP and enables crawling on a glass surface[67]. A molecular microrobot exhibiting amoeba-like body deformations can also be engineered using a lipid vesicle that contains proteins, kinesin molecular motors and microtubules. A DNA signal engages DNA clutches at the inside of the lipid membrane that anchors the kinesins, causing the microtubules to slide with respect to the membrane, thus generating forces, which cause membrane deformation. A light trigger disengages the DNA clutches and terminates the deformation of the molecular microrobot[68]. The cytoskeleton of the cell, which possesses unique out-of-equilibrium properties and can therefore be described as an 'active gel' (REF.[69]), plays a crucial role in amoeboid locomotion. The recreation of such an active matter system constitutes a key milestone to develop amoeboid and other autonomous microrobotic systems.

Autonomous and collective behaviours

Active matter systems allow the implementation of autonomous and collective behaviours in microrobots. The term active matter refers to systems that are composed of many self-driven units, with each unit capable of converting energy into movement[70]. Active matter

Box 1 | **Autonomy without reasoning**

Microrobots are unlikely to achieve a sufficient level of computational power to incorporate computer-based artificial intelligence. However, intelligent (autonomous) behaviours can be achieved without a reasoning unit or a 'conscious' representation of the world[114]. In a famous thought experiment, Braitenberg conceived vehicles that autonomously move under direct control of their sensors and without any central processing unit, yet exhibit complex and seemingly intelligent behaviours[115]. Analogously, microorganisms exhibit remarkable autonomous behaviours, such as locomotion and taxis, by reacting to external stimuli. Therefore, it should be possible to also implement a minimal level of intelligence in microrobots. Active particles exhibit basic collective and autonomous behaviours, but their behavioural complexity is not yet comparable to that of microorganisms.

The behaviours of microorganisms are a result of concurrent reactions to environmental stimuli. The robotic analogue is behaviour-based robotics, in which complex autonomous responses emerge from the interaction among different modules, or behaviours, each with a simple response to the environment[116–118] (for example, 'wander' or 'avoid obstacle'). Using this approach, complex autonomous behaviours can be implemented by providing the robot with a set of predefined simple stimuli-responsive behaviours and by defining their interactions. Autonomous microrobots (or microrobotic swarms) could be built with stimuli-responsive and/or active materials that interact with each other. Various stimuli-responsive materials and active particles have been developed; however, it remains challenging to design and tune their interactions to realize specific autonomous behaviours. This will enable microrobots to perform sophisticated tasks in complex environments despite the limited possibilities for external control.

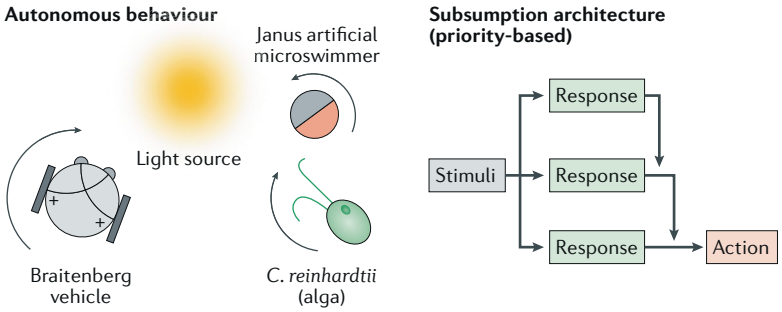

systems are ubiquitous at all scales in biology, including the cytoskeleton of living cells[71], bacterial suspensions, and terrestrial, aquatic and aerial flocks[70]. Active matter is defined by the following properties[72]: the energy input is local (at each unit level), and thus homogeneously distributed; the self-propelled motion is force free (forces that particles and fluid exert on each other cancel each other out); and the direction of motion is not constrained by an external field but is defined by the orientation of the unit itself. Non-living active matter systems include vibrated granular rods, self-propelled colloids and particles, and collections of robots[70]. Active matter systems enable self-propulsion, energetic autonomy, autonomous navigation guided by environmental cues and collective behaviours in microrobots[73].

Self-phoretic movement. Most active colloids move by self-phoretic effects. Phoresis is the movement of small particles and molecules in response to external gradients, such as temperature or concentration gradients[74]. Many analytical methods and separation technologies exploit particle phoresis, for example, the application of an electric field to charged analytes in gel electrophoresis[75]. The motive gradient can also be generated by the particle itself without the need for an external field, causing autonomous motion or 'self-phoresis' (REF.[76]) (FIG. 5a). For example, a particle can move in response to a locally generated thermal gradient (self-thermophoresis), as is observed for asymmetric Janus gold–silica particles that are illuminated with a near-infrared laser. Absorption primarily occurs on the gold side, which leads to a local temperature gradient in the surrounding fluid between the hotter gold side and the colder silica side[77]. Such a temperature gradient can either pull or push the particle, depending on the composition of the solution and the sign of the Soret coefficient, which is difficult to predict or compute[78]. Particle systems can also obtain their energy directly from the environment by converting chemical energy into mechanical energy, thus acting as chemical micromotors. Such self-phoretic catalytic systems show almost completely autonomous behaviour[79].

Catalytic micromotors and nanomotors. Many microorganisms harness chemical energy from their environment in the form of nutrients or prey. Analogously, catalytic micromotors and nanomotors self-propel by harnessing and converting chemical free energy (often a specific fuel, such as hydrogen peroxide, H_2O_2) into mechanical energy (motion)[80]. Directed motion is facilitated by asymmetric chemical reactivity rather than by moving parts[81], such that the shape of the particle, the location of the catalyst and the nature of the reaction dictate the type of propulsion. Asymmetric catalytic microstructures include bimetallic nanorods, in which redox reactions occur at both ends of the rod[82], coated Janus particles[83] and rolled-up microtubes[84]. The reactions occurring at the catalytic site generate propulsion, for example, by bubble propulsion or different self-phoretic effects[79].

A concentration gradient of reaction products and educts across the particle results in 'self-diffusiophoresis' (REF.[85–87]), that is, a phoretic movement induced by self-generated chemical gradients. For example, polystyrene microspheres can be half coated with platinum[83], which catalyses the decomposition of H_2O_2, leading to the generation of a local chemical gradient that induces the motion of the microspheres in the direction of the non-coated side. Electrokinetic effects also contribute to the autonomous propulsion of self-diffusiophoretic particles owing to imbalances in the charge distribution across the particle[75,88]. Self-electrophoresis also provides a propulsion mechanism for catalytic micromotors and nanomotors, such as bimetallic nanorods and nanorobots[89,90]. In such conducting nanomotors, H_2O_2 oxidation occurs at the platinum, end and its reduction occurs at the gold end, sustaining the propulsion of the nanostructure[91].

A non-phoretic catalytic mechanism for self-propulsion relies on the asymmetric generation and ejection of gas bubbles. Catalytic micromotors generate gaseous oxygen while consuming H_2O_2. If the particle has both high catalytic activity and a rough surface or if the generated gas accumulates in a confined space, as in microtubes, bubbles are released and push the micromotor[92]. For example, strain-engineered microtubes[84], which have an inner platinum surface that catalyses the decomposition of H_2O_2, move by bubble

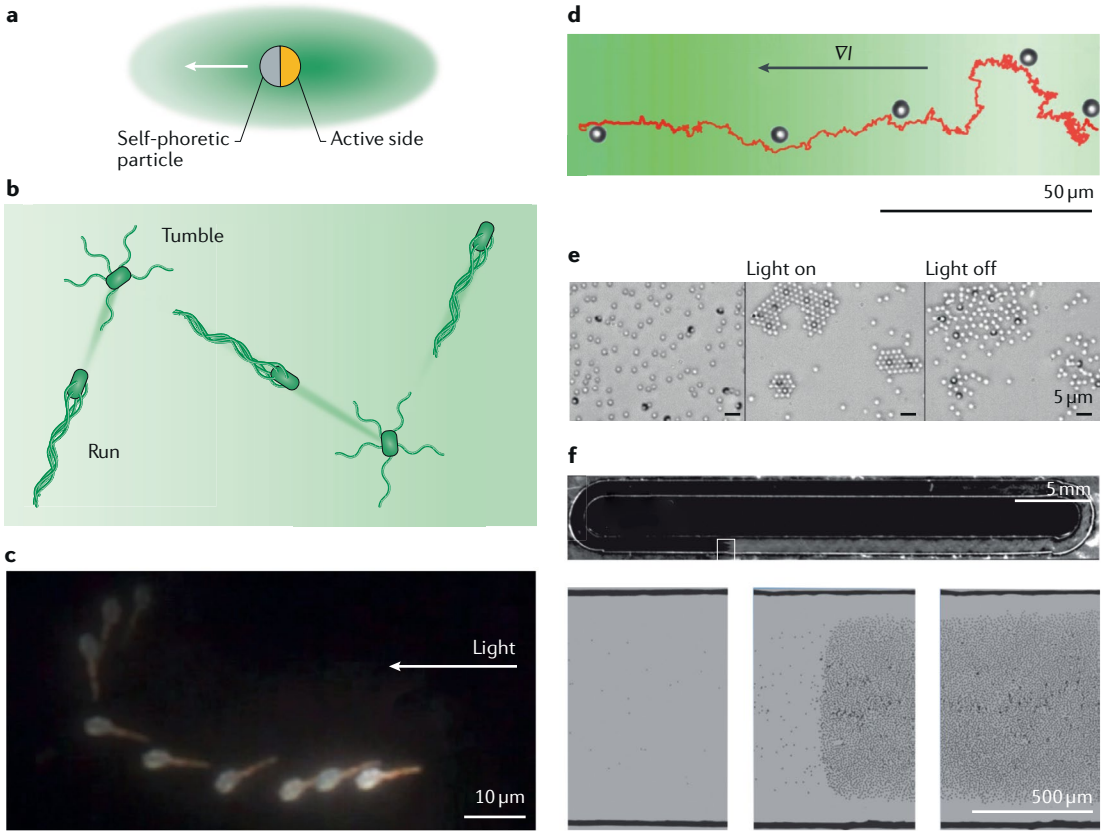

Fig. 5 | **Bioinspired autonomy. a** | Schematic of a self-phoretic Janus particle. The active side of the particle generates a physical or chemical gradient that induces motion of the particle. **b** | In bacteria, change of the direction of rotation of one flagellum causes the flagella to unbundle and the cell to tumble. The frequency of tumbling events is affected by molecules in the environment sensed by receptors, enabling chemotaxis[100]. **c** | Positive phototaxis of Janus catalytic nanotrees: under side illumination, the nanotrees experience asymmetric catalytic reaction speeds. **d** | Phototactic motion of carbon-coated Janus particles in a water–lutidine mixture exposed to a non-uniform light field: the tactic behaviour arises from an orientational response of the spherical active colloids to the light intensity gradient. **e** | Light-controlled crystal formation in a mixture of active–passive particles. Particles with a dark crescent or ring at the edge are light-activated self-phoretic particles. **f** | Quincke rollers spontaneously form a macroscopic band propagating along a racetrack. The bottom pictures represent the isotropic gas phase, the propagating band and the homogeneous polar liquid phase, respectively. ∇*I*, gradient. Panel **c** is adapted from REF.[104], CC-BY-4.0. Panel **d** is adapted from REF.[103], Macmillan Publishers Limited. Panel **e** is adapted with permission from REF.[111], John Wiley and Sons. Panel **f** is adapted from REF.[112], Macmillan Publishers Limited.

propulsion. The microtubes are slightly conical, allowing the bubbles to escape from the wider opening, pushing the tube forward[93].

The chemical reactions exploited for propulsion often require toxic fuels, such as H_2O_2. Therefore, biocompatible reactions[94], such as enzymatic reactions[95], which integrate a response to naturally occurring enzyme substrates, acid-driven propulsion[96] and photocatalytic reactions in pure water[97,98], are currently being explored as drivers for propulsion.

Self-phoretic particles are not only interesting because of their motility but also because they can exhibit collective behaviours[73,99] and they can respond to environmental cues, such as concentration gradients.

Artificial taxis. In biology, the term 'taxis' refers to the ability of an organism to sense and respond to an external stimulus with biased movement, for example, by actively orienting itself in response to a concentration gradient (chemotaxis), to gravitational forces (gravitaxis), to the flow of the surrounding fluid (rheotaxis), to a magnetic field (magnetotaxis) or to light (phototaxis). Bacteria have surface receptors that sense molecules in the environment and allow them to follow chemical cues. In response to specific molecules, bacteria can stall or even briefly change the direction of rotation of the flagellar motors, thus unbundling the flagella and causing a reorientation of the body. Motion in the direction of the higher concentration of a chemical attractant thus results in long straight 'runs' and less orientation 'tumbles', enabling the cells to find favourable conditions[100] (FIG. 5b). Bacteria are generally too small to perceive differences in the physical and chemical stimuli across their body (spatial comparison). They are nonetheless able to evaluate the direction of physical and chemical gradients by sensing the environmental conditions at different times as they move (temporal comparison). The perceived environmental stimuli then indirectly guide the bacteria, that is, the intensity of the stimulus modulates the probability of turning,

resulting in a biased random walk. Unicellular algae such as *Chlamydomonas reinhardtii* respond to light by performing temporal comparison with direct guiding because their photosensor allows them to perceive the direction of light[101].

Self-phoretic particles can exhibit behaviours resembling biological taxis in response to an external field or stimulus that biases their rotational Brownian motion[75]. For example, phoretic particles can migrate upstream against a pressure-driven fluid flow (positive rheotaxis)[102]. Flow-induced torque leads to alignment of the asymmetric particles, resulting in directed locomotion. Light-driven self-electrophoretic Janus nanotrees also exhibit positive or negative phototaxis, depending on the surface functionalization. The nanotrees, unlike one-dimensional nanowires, can sense the direction of the incoming light through absorption mainly perpendicular to their main axis, which leads to the asymmetric generation of photoelectrochemical reaction products and thus an effective torque on the nanotree[103] (FIG. 5c). Phototactic motion has been observed for spherical self-propelled particles in non-uniform light fields, in which the particles move towards regions of lower light intensity[104] (FIG. 5d). Chemotactic microrobots are envisioned to be able to perceive specific chemical cues expressed, for example, by a tumour and to autonomously move on the basis of the chemical gradient. For example, biohybrid microrobots containing bacteria spontaneously align along chemical cues[105] and find and accumulate in hypoxic tumour regions[106]. However, realizing fully artificial systems that are biocompatible and that are able to follow specific chemical cues in the environment remains a challenge. Active particles and microrobots do not only respond to their chemical environment but also interact with each other and thus give rise to collective behaviours.

Collective behaviours. Biological microswimmers within dense or semi-dilute cell populations hydrodynamically interact with each other. Each cell generates a flow field that is felt by surrounding cells, causing aligning interactions[9]. Swimming microorganisms can be considered polar self-propelled particles, whose interactions can result either in a state with nematic (apolar) order, with zero average speed, or with polar order, having a non-zero average speed[70]. These interactions result in collective motion and swarm formation that are characteristic for many active matter systems

Artificial self-propelled particles also interact with each other and exhibit collective behaviours[107]. These interactions can occur at different length scales and result either in attraction or repulsion[108]. Therefore, collective behaviours depend on the activity and density of the particles[99]. For example, carbon-coated Janus particles that self-propel in a water–lutidine mixture near the critical point cluster, leading to phase separation. In this system, the influence of attractive forces is suppressed; hence, clustering is caused by dynamic self-trapping. Phase separation into a crystal-like and a gas-like phase also occurs when the density of this active colloidal suspension is further increased[109]. Similarly, clustering can be observed in populations of photocatalytic colloids that consist of polymer microspheres, which display an antiferromagnetic haematite cube on one side. Immersion in H_2O_2 and activation by blue light triggers self-propulsion of the particles, and above a certain density threshold, the particles assemble into dynamic clusters[110]. Light activation of self-phoretic colloids can be used to induce crystallization of passive silica particles. A small number of self-propelled photocatalytic colloids are sufficient to direct the dynamic and controlled crystallization of passive particles into 2D assemblies[111] (FIG. 5e). Collective directed motion has been observed in confined populations of dielectric particles that are exposed to a static electric field. These Quincke rollers start to rotate along an axis perpendicular to the applied field, leading to translational motion if the particles are close to a solid boundary. At high densities, the particles organize and collectively move in one direction[112,113] (FIG. 5f).

Such chemically and externally driven active systems exhibit autonomous motion and collective behaviours showing parallels to the organization of flocks of birds, schools of fishes, bacterial colonies or proteins in the cytoskeleton of cells[72]. Active materials can thus equip the next generation of microrobots with autonomy and, eventually, intelligence (BOX 1).

Conclusions and outlook

Unicellular microorganisms, such as bacteria, are among the simplest life forms on earth. Microorganisms have no central nervous system, yet they show 'intelligent' behaviours and perform remarkable tasks, such as locomotion in liquids and solids, sensing and directed motion, interaction with the environment and collective behaviours. Mimicking biological microorganisms offers the possibility to realize artificial robots at the microscale. Microrobots are too small to be built with traditional hardware and therefore special material systems are required to implement actuation, control and sensing at the microscale. Soft, responsive and active material systems are central to the development of microscale robots, enabling controlled locomotion, specific functionalities, such as delivery and release of molecules, responses to environmental changes and autonomous operation.

The field of microrobotics strives to design fully artificial intelligent microrobots that are functional and autonomous. Externally controlled microrobots could also benefit from some degree of autonomy because microrobots can exchange only limited information with the outside world. Autonomy facilitates miniaturization, allows for long operating times and enables the implementation of simple robotic units that collectively interact and, thus, enable complex emergent behaviours. Responsive and active materials are key in realizing autonomous behaviour because of their inherent capability to sense the environment and act in response to external stimuli. Materials have been developed that could in principle be used to enable the integration of sensing and actuation in microrobots, as well as efficient energy conversion and the ability to respond to the environment and act (semi-)autonomously. The main

challenge in the quest to develop intelligent microrobots lies in the functional integration of different material systems in a microscopic device. This will require a deep understanding of the material response and a holistic design of the microrobotic system, which can benefit from advanced material simulations and from taking inspiration from biological organisms. This endeavour will not only lead to the next generation of advanced microrobots but also aid the development of intelligent material systems, providing the opportunity to advance a number of fields, including microsurgery and targeted drug delivery.

Published online 10 May 2018

1. Dusenbery, D. B. Minimum size limit for useful locomotion by free-swimming microbes. *Proc. Natl Acad. Sci. USA* **94**, 10949–10954 (1997).
2. Feynman, R. P. There's plenty of room at the bottom. *Engineer. Sci.* **23**, 22–36 (1960).
3. Nelson, B. J., Kaliakatsos, I. K. & Abbott, J. J. Microrobots for minimally invasive medicine. *Annu. Rev. Biomed. Eng.* **12**, 55–85 (2010).
4. Li, J., Esteban-Fernández de Ávila, B., Gao, W., Zhang, L. & Wang, J. Micro/nanorobots for biomedicine: delivery, surgery, sensing, and detoxification. *Sci. Robot.* **2**, eaam6431 (2017).
5. Purcell, E. M. Life at low Reynolds number. *Am. J. Phys.* **45**, 3–11 (1977).
6. Palagi, S., Walker, D., Qiu, T. & Fischer, P. in *Microbiorobotics* 2nd edn (eds Kim, M., Julius, A. A. & Cheang, U. K.) 133–162 (Elsevier, 2017).
7. Qiu, T. et al. Swimming by reciprocal motion at low Reynolds number. *Nat. Commun.* **5**, 5119 (2014).
8. Venugopalan, P. L. et al. Conformal cytocompatible ferrite coatings facilitate the realization of a nanovoyager in human blood. *Nano Lett.* **14**, 1968–1975 (2014).
9. Lauga, E. & Powers, T. R. The hydrodynamics of swimming microorganisms. *Rep. Prog. Phys.* **72**, 96601 (2009).
10. Behkam, B. & Sitti, M. Design methodology for biomimetic propulsion of miniature swimming robots. *J. Dynam. Syst. Meas. Control* **128**, 36–43 (2006).
11. Fischer, P. & Ghosh, A. Magnetically actuated propulsion at low Reynolds numbers: towards nanoscale control. *Nanoscale* **3**, 557–563 (2011).
12. Jarrell, K. F. & McBride, M. J. The surprisingly diverse ways that prokaryotes move. *Nat. Rev. Microbiol.* **6**, 466–476 (2008).
13. Bray, D. *Cell Movements: From Molecules to Motility*. 2nd edn (Garland Science, 2001).
14. Walker, D., Kübler, M., Morozov, K. I., Fischer, P. & Leshansky, A. M. Optimal length of low Reynolds number nanopropellers. *Nano Lett.* **15**, 4412–4416 (2015).
15. Zhang, L. et al. Artificial bacterial flagella: fabrication and magnetic control. *Appl. Phys. Lett.* **94**, 64103–64107 (2009).
16. Ghosh, A. & Fischer, P. Controlled propulsion of artificial magnetic nanostructured propellers. *Nano Lett.* **9**, 2243–2245 (2009).
17. Schamel, D. et al. Nanopropellers and their actuation in complex viscoelastic media. *ACS Nano* **8**, 8794–8801 (2014).
18. Li, J. et al. Template electrosynthesis of tailored-made helical nanoswimmers. *Nanoscale* **6**, 9415–9420 (2014).
19. Tottori, S. et al. Magnetic helical micromachines: fabrication, controlled swimming, and cargo transport. *Adv. Mater.* **24**, 811–816 (2012).
20. Gao, W. et al. Bioinspired helical microswimmers based on vascular plants. *Nano Lett.* **14**, 305–310 (2014).
21. Yan, X. et al. Multifunctional biohybrid magnetite microrobots for imaging-guided therapy. *Sci. Robot.* **2**, eaaq1155 (2017).
22. Walker, D., Käsdorf, B. T., Jeong, H.-H., Lieleg, O. & Fischer, P. Enzymatically active biomimetic micropropellers for the penetration of mucin gels. *Sci. Adv.* **1**, e1500501 (2015).
23. Huang, H. W., Chao, Q., Sakar, M. S. & Nelson, B. J. Optimization of tail geometry for the propulsion of soft microrobots. *IEEE Robot. Autom. Lett.* **2**, 727–732 (2017).
24. Maier, A. M. et al. Magnetic propulsion of microswimmers with DNA-based flagellar bundles. *Nano Lett.* **16**, 906–910 (2016).
25. Ishijima, S. Mechanical constraint converts planar waves into helices on tunicate and sea urchin sperm flagella. *Cell Struct. Funct.* **37**, 13–19 (2012).
26. Abbott, J. J. et al. How should microrobots swim? *Int. J. Robot. Res.* **28**, 1434–1447 (2009).
27. Lagomarsino, M. C., Capuani, F. & Lowe, C. P. A simulation study of the dynamics of a driven filament in an Aristotelian fluid. *J. Theor. Biol.* **224**, 215–224 (2003).
28. Pak, O. S., Gao, W., Wang, J. & Lauga, E. High-speed propulsion of flexible nanowire motors: theory and experiments. *Soft Matter* **7**, 8169–8181 (2011).
29. Khalil, I. S. M., Tabak, A. F., Klingner, A. & Sitti, M. Magnetic propulsion of robotic sperms at low-Reynolds number. *Appl. Phys. Lett.* **109**, 033701 (2016).
30. Williams, B. J., Anand, S. V., Rajagopalan, J. & Saif, M. T. A. A self-propelled biohybrid swimmer at low Reynolds number. *Nat. Commun.* **5**, 3081 (2014).
31. Dreyfus, R. et al. Microscopic artificial swimmers. *Nature* **437**, 862–865 (2005).
32. Roper, M. et al. Do magnetic micro-swimmers move like eukaryotic cells? *Proc. R. Soc. A Math. Phys. Engineer. Sci.* **464**, 877–904 (2008).
33. Li, T. et al. Magnetically propelled fish-like nanoswimmers. *Small* **12**, 6098–6105 (2016).
34. Diller, E., Zhuang, J., Zhan Lum, G., Edwards, M. R. & Sitti, M. Continuously distributed magnetization profile for millimeter-scale elastomeric undulatory swimming. *Appl. Phys. Lett.* **104**, 174101 (2014).
35. Hu, W., Lum, G. Z., Mastrangeli, M. & Sitti, M. Small-scale soft-bodied robot with multimodal locomotion. *Nature* **554**, 81 (2018).
36. Evans, B. A. et al. Magnetically actuated nanorod arrays as biomimetic cilia. *Nano Lett.* **7**, 1428–1434 (2007).
37. Shields, A. R. et al. Biomimetic cilia arrays generate simultaneous pumping and mixing regimes. *Proc. Natl Acad. Sci. USA* **107**, 15670–15675 (2010).
38. Elgeti, J. & Gompper, G. Emergence of metachronal waves in cilia arrays. *Proc. Natl Acad. Sci. USA* **110**, 4470–4475 (2013).
39. Yan, X., Wang, F., Zheng, B. & Huang, F. Stimuli-responsive supramolecular polymeric materials. *Chem. Soc. Rev.* **41**, 6042–6065 (2012).
40. Zeng, H., Wasylczyk, P., Wiersma, D. S. & Priimagi, A. Light robots: bridging the gap between microrobotics and photomechanics in soft materials. *Adv. Mater.* https://doi.org/10.1002/adma.201703554 (2017).
41. Ohm, C., Brehmer, M. & Zentel, R. Liquid crystalline elastomers as actuators and sensors. *Adv. Mater.* **22**, 3366–3387 (2010).
42. Palagi, S. et al. Structured light enables biomimetic swimming and versatile locomotion of photoresponsive soft microrobots. *Nat. Mater.* **15**, 647–653 (2016).
43. Huang, H.-W., Sakar, M. S., Petruska, A. J., Pane, S. & Nelson, B. J. Soft micromachines with programmable motility and morphology. *Nat. Commun.* **7**, 12263 (2016).
44. Wang, W. et al. Thermo-driven microcrawlers fabricated via a microfluidic approach. *J. Phys. D Appl. Phys.* **46**, 114007 (2013).
45. Mourran, A., Zhang, H., Vinokur, R. & Möller, M. Soft microrobots employing nonequilibrium actuation via plasmonic heating. *Adv. Mater.* **29**, 1604825 (2017).
46. Govorov, A. O. & Richardson, H. H. Generating heat with metal nanoparticles. *Nano Today* **2**, 30–38 (2007).
47. Camacho-Lopez, M., Finkelmann, H., Palffy-Muhoray, P. & Shelley, M. Fast liquid-crystal elastomer swims into the dark. *Nat. Mater.* **3**, 307–310 (2004).
48. Zeng, H. et al. Light-fueled microscopic walkers. *Adv. Mater.* **27**, 3883–3887 (2015).
49. Palima, D. & Glückstad, J. Gearing up for optical microrobotics: micromanipulation and actuation of synthetic microstructures by optical forces. *Laser Photon. Rev.* **7**, 478–494 (2013).
50. Blake, J. R. A spherical envelope approach to ciliary propulsion. *J. Fluid Mech.* **46**, 199–208 (1971).
51. Childress, S. *Mechanics of Swimming and Flying*. Vol. 2 (Cambridge Univ. Press, 1981).
52. Palagi, S., Jager, E. W. H., Mazzolai, B. & Beccai, L. Propulsion of swimming microrobots inspired by metachronal waves in ciliates: from biology to material specifications. *Bioinspir. Biomimet.* **8**, 46004 (2013).
53. Palagi, S. et al. in *2016 International Conference on Manipulation, Automation and Robotics at Small Scales (MARSS)* (Paris, France, 2016).
54. Palagi, S. et al. in *2017 International Conference on Manipulation, Automation and Robotics at Small Scales (MARSS)* (Montreal, Canada, 2017).
55. Magdanz, V., Guix, M., Hebenstreit, F. & Schmidt, O. G. Dynamic polymeric microtubes for the remote-controlled capture, guidance, and release of sperm cells. *Adv. Mater.* **28**, 4084–4089 (2016).
56. Breger, J. C. et al. Self-folding thermo-magnetically responsive soft microgrippers. *ACS Appl. Mater. Interfaces* **7**, 3398–3405 (2015).
57. Iacovacci, V. et al. Untethered magnetic millirobot for targeted drug delivery. *Biomed. Microdevices* **17**, 1–12 (2015).
58. Tabatabaei, S. N., Lapointe, J. & Martel, S. Shrinkable hydrogel-based magnetic microrobots for interventions in the vascular network. *Adv. Robot.* **25**, 1049–1067 (2011).
59. Fusco, S. et al. Shape-switching microrobots for medical applications: the influence of shape in drug delivery and locomotion. *ACS Appl. Mater. Interfaces* **7**, 6803–6811 (2015).
60. Fusco, S. et al. Chitosan electrodeposition for microrobotic drug delivery. *Adv. Healthc. Mater.* **2**, 1037–1044 (2013).
61. Li, H., Go, G., Ko, S. Y., Park, J.-O. & Park, S. Magnetic actuated pH-responsive hydrogel-based soft micro-robot for targeted drug delivery. *Smart Mater. Struct.* **25**, 027001 (2016).
62. Yoshida, R. Self-oscillating polymer gel as novel biomimetic materials exhibiting spatiotemporal structure. *Colloid. Polym. Sci.* **289**, 475–487 (2011).
63. Maeda, S., Hara, Y., Sakai, T., Yoshida, R. & Hashimoto, S. Self-walking gel. *Adv. Mater.* **19**, 3480–3484 (2007).
64. Piovanelli, M., Fujie, T., Mazzolai, B. & Beccai, L. in *2012 4th IEEE RAS & EMBS International Conference on Biomedical Robotics and Biomechatronics (BioRob)* 612–616 (Rome, Italy, 2012).
65. Lämmermann, T. & Sixt, M. Mechanical modes of 'amoeboid' cell migration. *Curr. Opin. Cell Biol.* **21**, 636–644 (2009).
66. Onoda, M., Ueki, T., Tamate, R., Shibayama, M. & Yoshida, R. Amoeba-like self-oscillating polymeric fluids with autonomous sol-gel transition. *Nat. Commun.* **8**, 15862 (2017).
67. Yi, J., Schmidt, J., Chien, A. & Montemagno, C. D. Engineering an artificial amoeba propelled by nanoparticle-triggered actin polymerization. *Nanotechnology* **20**, 085101 (2009).
68. Sato, Y., Hiratsuka, Y., Kawamata, I., Murata, S. & Nomura, S.-i.M. Micrometer-sized molecular robot changes its shape in response to signal molecules. *Sci. Robot.* **2**, eaal3735 (2017).
69. Terentjev, E. M. & Weitz, D. A. *The Oxford Handbook of Soft Condensed Matter*. (Oxford Univ. Press, 2015).
70. Marchetti, M. C. et al. Hydrodynamics of soft active matter. *Rev. Mod. Phys.* **85**, 1143 (2013).
71. Needleman, D. & Dogic, Z. Active matter at the interface between materials science and cell biology. *Nat. Rev. Mater.* **2**, 17048 (2017).
72. Ramaswamy, S. The mechanics and statistics of active matter. *Annu. Rev. Condens. Matter Phys.* **1**, 323–345 (2010).
73. Illien, P., Golestanian, R. & Sen, A. 'Fuelled' motion: phoretic motility and collective behaviour of active colloids. *Chem. Soc. Rev.* **46**, 5508–5518 (2017).
74. Anderson, J. L. Colloid transport by interfacial forces. *Annu. Rev. Fluid Mechan.* **21**, 61–99 (1989).

75. Moran, J. L. & Posner, J. D. Phoretic self-propulsion. *Annu. Rev. Fluid Mechan.* **49**, 511–540 (2017).
76. Bechinger, C. et al. Active particles in complex and crowded environments. *Rev. Mod. Phys.* **88**, 045006 (2016).
77. Jiang, H.-R., Yoshinaga, N. & Sano, M. Active motion of a Janus particle by self-thermophoresis in a defocused laser beam. *Phys. Rev. Lett.* **105**, 268302 (2010).
78. Ning, H., Buitenhuis, J., Dhont, J. K. G. & Wiegand, S. Thermal diffusion behavior of hard-sphere suspensions. *J. Chem. Phys.* **125**, 204911 (2006).
79. Paxton, W. F., Sundararajan, S., Mallouk, T. E. & Sen, A. Chemical locomotion. *Angew. Chem. Int. Ed.* **45**, 5420–5429 (2006).
80. Sánchez, S., Soler, L. & Katuri, J. Chemically powered micro- and nanomotors. *Angew. Chem. Int. Ed.* **54**, 1414–1444 (2015).
81. Kapral, R. Perspective: Nanomotors without moving parts that propel themselves in solution. *J. Chem. Phys.* **138**, 020901 (2013).
82. Paxton, W. F. et al. Catalytic nanomotors: autonomous movement of striped nanorods. *J. Am. Chem. Soc.* **126**, 13424–13431 (2004).
83. Howse, J. R. et al. Self-motile colloidal particles: from directed propulsion to random walk. *Phys. Rev. Lett.* **99**, 048102 (2007).
84. Solovev, A. A., Mei, Y., Bermúdez Ureña, E., Huang, G. & Schmidt, O. G. Catalytic microtubular jet engines self-propelled by accumulated gas bubbles. *Small* **5**, 1688–1692 (2009).
85. Golestanian, R., Liverpool, T. B. & Ajdari, A. Propulsion of a molecular machine by asymmetric distribution of reaction products. *Phys. Rev. Lett.* **94**, 220801 (2005).
86. Popescu, M. N., Uspal, W. E. & Dietrich, S. Self-diffusiophoresis of chemically active colloids. *Eur. Phys. J. Special Top.* **225**, 2189–2206 (2016).
87. Uspal, W. E., Popescu, M. N., Dietrich, S. & Tasinkevych, M. Guiding catalytically active particles with chemically patterned surfaces. *Phys. Rev. Lett.* **117**, 048002 (2016).
88. Brown, A. & Poon, W. Ionic effects in self-propelled Pt-coated Janus swimmers. *Soft Matter* **10**, 4016–4027 (2014).
89. Paxton, W. F., Sen, A. & Mallouk, T. E. Motility of catalytic nanoparticles through self-generated forces. *Chem. Eur. J.* **11**, 6462–6470 (2005).
90. Chen, K. et al. "Z"-shaped rotational Au/Pt micro-nanorobot. *Micromachines* **8**, 183 (2017).
91. Wang, Y. et al. Bipolar electrochemical mechanism for the propulsion of catalytic nanomotors in hydrogen peroxide solutions. *Langmuir* **22**, 10451–10456 (2006).
92. Wang, S. & Wu, N. Selecting the swimming mechanisms of colloidal particles: bubble propulsion versus self-diffusiophoresis. *Langmuir* **30**, 3477–3486 (2014).
93. Fomin, V. M. et al. Propulsion mechanism of catalytic microjet engines. *IEEE Trans. Robot.* **30**, 40–48 (2014).
94. Abdelmohsen, L. K. E. A., Peng, F., Tu, Y. & Wilson, D. A. Micro- and nano-motors for biomedical applications. *J. Mater. Chem. B* **2**, 2395–2408 (2014).
95. Abdelmohsen, L. K. E. A. et al. Dynamic loading and unloading of proteins in polymeric stomatocytes: formation of an enzyme-loaded supramolecular nanomotor. *ACS Nano* **10**, 2652–2660 (2016).
96. Gao, W. et al. Artificial micromotors in the mouse's stomach: a step toward in vivo use of synthetic motors. *ACS Nano* **9**, 117–123 (2015).
97. Dong, R., Zhang, Q., Gao, W., Pei, A. & Ren, B. Highly efficient light-driven TiO2–Au Janus micromotors. *ACS Nano* **10**, 839–844 (2016).
98. Dong, R. et al. Visible-light-driven BiOI-based Janus micromotor in pure water. *J. Am. Chem. Soc.* **139**, 1722–1725 (2017).
99. Pohl, O. & Stark, H. Dynamic clustering and chemotactic collapse of self-phoretic active particles. *Phys. Rev. Lett.* **112**, 238303 (2014).
100. Berg, H. C. The rotary motor of bacterial flagella. *Annu. Rev. Biochem.* **72**, 19–54 (2003).
101. Dusenbery, D. B. *Living at Micro Scale: The Unexpected Physics of Being Small*. (Harvard Univ. Press, 2009).
102. Palacci, J. et al. Artificial rheotaxis. *Sci. Adv.* **1**, e1400214 (2015).
103. Dai, B. et al. Programmable artificial phototactic microswimmer. *Nat. Nanotechnol* **11**, 1087–1092 (2016).
104. Lozano, C., ten Hagen, B., Löwen, H. & Bechinger, C. Phototaxis of synthetic microswimmers in optical landscapes. *Nat. Commun.* **7**, 12828 (2016).
105. Zhuang, J. & Sitti, M. Chemotaxis of bio-hybrid multiple bacteria-driven microswimmers. *Sci. Rep.* **6**, 32135 (2016).
106. Felfoul, O. et al. Magneto-aerotactic bacteria deliver drug-containing nanoliposomes to tumour hypoxic regions. *Nat. Nanotechnol.* **11**, 941–947 (2016).
107. Wang, W., Duan, W., Sen, A. & Mallouk, T. E. Catalytically powered dynamic assembly of rod-shaped nanomotors and passive tracer particles. *Proc. Natl Acad. Sci. USA* **110**, 17744–17749 (2013).
108. Nourhani, A., Brown, D., Pletzer, N. & Gibbs, J. G. Engineering contactless particle–particle interactions in active microswimmers. *Adv. Mater.* **29**, 1703910 (2017).
109. Buttinoni, I. et al. Dynamical clustering and phase separation in suspensions of self-propelled colloidal particles. *Phys. Rev. Lett.* **110**, 238301 (2013).
110. Palacci, J., Sacanna, S., Steinberg, A. P., Pine, D. J. & Chaikin, P. M. Living crystals of light-activated colloidal surfers. *Science* **339**, 936–940 (2013).
111. Singh, D. P., Choudhury, U., Fischer, P. & Mark, A. G. Non-equilibrium assembly of light-activated colloidal mixtures. *Adv. Mater.* **29**, 1701328 (2017).
112. Bricard, A., Caussin, J.-B., Desreumaux, N., Dauchot, O. & Bartolo, D. Emergence of macroscopic directed motion in populations of motile colloids. *Nature* **503**, 95–98 (2013).
113. Yan, J. et al. Reconfiguring active particles by electrostatic imbalance. *Nat. Mater.* **15**, 1095 (2016).
114. Brooks, R. A. Intelligence without representation. *Artif. Intell.* **47**, 139–159 (1991).
115. Braitenberg, V. *Vehicles: Experiments in Synthetic Psychology* (MIT Press, 1986).
116. Brooks, R. A. *Cambrian Intelligence: The Early History of the New AI* (MIT Press, 1999).
117. Brooks, R. A. & Connell, J. H. in *Proceedings of SPIE* https://doi.org/10.1117/12.937785 (1987).
118. Murphy, R. *Introduction to AI Robotics* (MIT Press, 2000).

Acknowledgements
The authors acknowledge helpful discussions with D. Singh and M. Popescu.

Author contributions
All authors contributed equally to the preparation of this manuscript.

Competing interests
The authors declare no competing interests.

Publisher's note
Springer Nature remains neutral with regard to jurisdictional claims in published maps and institutional affiliations.